BIOCATALYSIS

Photoexcitation of flavoenzymes enables a stereoselective radical cyclization

Kyle F. Biegasiewicz[1]*, Simon J. Cooper[1]*, Xin Gao[1]*, Daniel G. Oblinsky[1], Ji Hye Kim[1], Samuel E. Garfinkle[1], Leo A. Joyce[2], Braddock A. Sandoval[1], Gregory D. Scholes[1], Todd K. Hyster[1]†

Photoexcitation is a common strategy for initiating radical reactions in chemical synthesis. We found that photoexcitation of flavin-dependent "ene"-reductases changes their catalytic function, enabling these enzymes to promote an asymmetric radical cyclization. This reactivity enables the construction of five-, six-, seven-, and eight-membered lactams with stereochemical preference conferred by the enzyme active site. After formation of a prochiral radical, the enzyme guides the delivery of a hydrogen atom from flavin—a challenging feat for small-molecule chemical reagents. The initial electron transfer occurs through direct excitation of an electron donor-acceptor complex that forms between the substrate and the reduced flavin cofactor within the enzyme active site. Photoexcitation of promiscuous flavoenzymes has thus furnished a previously unknown biocatalytic reaction.

Radical enzymes catalyze radical-mediated reactions with exquisite chemo-, regio-, and enantioselectivity (*1*). These catalysts, however, exploit strategies for radical formation that do not translate well outside of the natural setting and thus do not lend themselves readily to be harnessed for robust synthetic organic chemistry, in which operational simplicity, generality, and ease of reaction execution are desirable (*2*). To achieve these features, it would be attractive to develop biocatalytic reactions that use mechanisms of radical formation commonly used in chemical synthesis. If these mechanisms were to occur within active sites of established enzymatic platforms known to be substrate promiscuous, general catalysts for asymmetric radical reactions could be accessed. Moreover, by repurposing known enzymes, desired biocatalytic functions can be achieved while retaining characteristics such as ease of handling, substrate promiscuity, and evolvability already associated with these catalysts (*3*).

Photoexcitation is widely used in organic synthesis to facilitate radical reactions (*4*) but is less common in enzyme catalysis. Light has been used to activate enzymes through conformational changes (*5*), drive charge separation in multiprotein systems (*6*), and facilitate cofactor turnover or substrate epimerization (*7*). Direct use of photonic energy to drive native, biological reactions is much more limited but has been documented for protochlorophyllide reductase (*8*), fatty acid photodecarboxylase (*9*), and DNA photolyase (*10*). We recently found that nicotinamide-dependent ketoreductases (KREDs) and double-bond reductases (DBRs) can use photoinduced electron transfer to effect asymmetric radical hydrodehalogenation and hydrodeacetoxylation reactions (*11*, *12*). These examples illustrate that irradiation of common oxidoreductases can draw out a non-natural reaction mode for catalysis, a feature we anticipate can be exploited to address challenges in chemical synthesis.

The stereoselective coupling of electrophilic radicals and unactivated alkenes enables the

[1]Department of Chemistry, Princeton University, Princeton, NJ 08544, USA. [2]Department of Process Research and Development, Merck, Rahway, NJ 07065, USA.
*These authors contributed equally to this work.
†Corresponding author. Email: thyster@princeton.edu

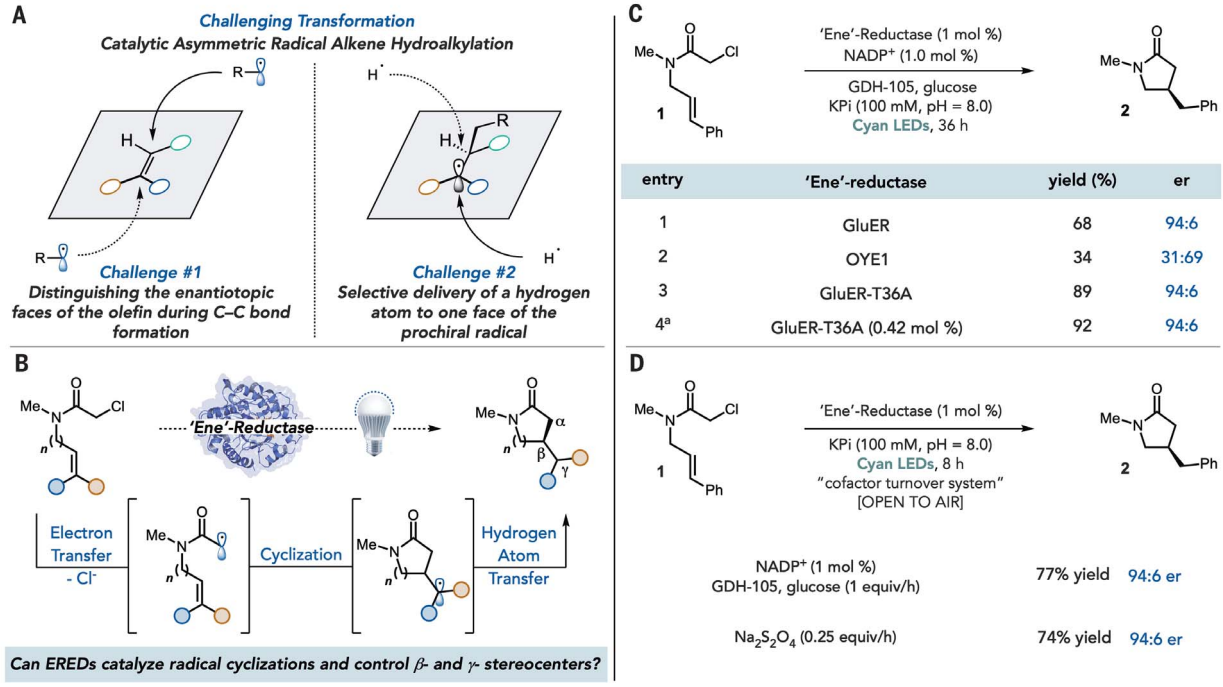

Fig. 1. Strategy for achieving a biocatalytic radical-mediated C–C bond formation. (**A**) Challenges associated with achieving a catalytic asymmetric radical hydroalkylation. (**B**) Proposed catalytic cycle for the biocatalytic radical cyclization to set β- and γ- positions. (**C**) Enzyme screen and optimization by means of mutagenesis. [a]Reaction run by using cell free lysate on 1-g scale. (**D**) Reaction conditions and results for running this reaction open to air.

preparation of structural motifs found in agrochemical and pharmaceutical agents (*13*). Catalytic strategies for rendering this type of transformation stereoselective remain elusive (*14*). This is primarily because of the challenge of maintaining association between radical species and chiral catalysts throughout the stereoselectivity-determining step and the lack of reagents capable of supplying a hydrogen atom to one face of a prochiral radical (Fig. 1A) (*15*). Given these challenges, we imagined that enzymes would be an ideal catalyst for this transformation because of their ability to precisely control the conformational landscape of reactive species. As a model for this family of reactivity, we targeted the development of a biocatalytic radical cyclization of α-chloroamides to afford β-stereogenic lactams (Fig. 1B). The lactam motif is prevalent in medicinally valuable molecules (*16*), and the proposed synthesis would be distinct from existing biocatalytic approaches for generating *N*-heterocycles (*17*). Although this cyclization is well known in the radical literature, it is plagued by preferential formation of the hydrodehalogenated and oligomerized product, and there are no known catalytic asymmetric variants (*18*, *19*). New enzymatic Csp^3–Csp^3 bond–forming reactions are desired in biocatalysis (*20*, *21*).

We looked to flavin-dependent "ene"-reductases (EREDs) as a potential catalyst family for the proposed cyclization of α-chloroamides. Because EREDs have large, substrate-promiscuous active sites, we hypothesized that these enzymes would be able to bind the substrate in a conformation to enable cyclization (*22*, *23*). Moreover, our recent studies demonstrated that these enzymes are able to control the stereochemical outcome of radical hydrodehalogenation reactions (*24*). Unfortunately, flavin hydroquinone (FMN_{hq}) is a modest single-electron reductant [$E_{1/2}$ = −0.45 V versus saturated calomel electrode (SCE)], making electron transfer to α-chloroamides ($E_{p/2}^{red}$ = −1.65 V versus SCE) thermodynamically challenging (fig. S23). The excited state of the flavin hydroquinone (FMN_{hq}*) ($E_{1/2}$* = −2.26 V versus SCE), however, should be capable of accomplishing this initial electron transfer (*25*). Previous work has investigated the fundamental photophysics of the FMN_{hq}* in flavin-dependent enzymes (*26*, *27*). If this excited state could be used for the envisioned chemistry, it would transform flavin-dependent enzymes into chiral photocatalysis the envisioned chemistry, substantially expanding their synthetic utility.

We began by testing the cyclization of α-chloroacetamide **1** to afford γ-lactam **2** under visible light irradiation (table S1). An ERED from *Gluconobacter oxydans* (GluER) was effective when irradiated with near–ultraviolet (UV) light (390 nm), furnishing the desired cyclization product with modest yield and enantioselectivity (table S2). Optimization of the lighting source revealed cyan light (497 nm) to provide product with improved yield and enantioselectivity while producing less than 2% of hydrodehalogenation product (Fig. 1C, entry 1). The opposite enantiomer is favored by Old Yellow Enzyme 1 (OYE1) (Fig. 1C, entry 2). Control experiments confirm that light, ERED, nicotinamide adenine dinucleotide

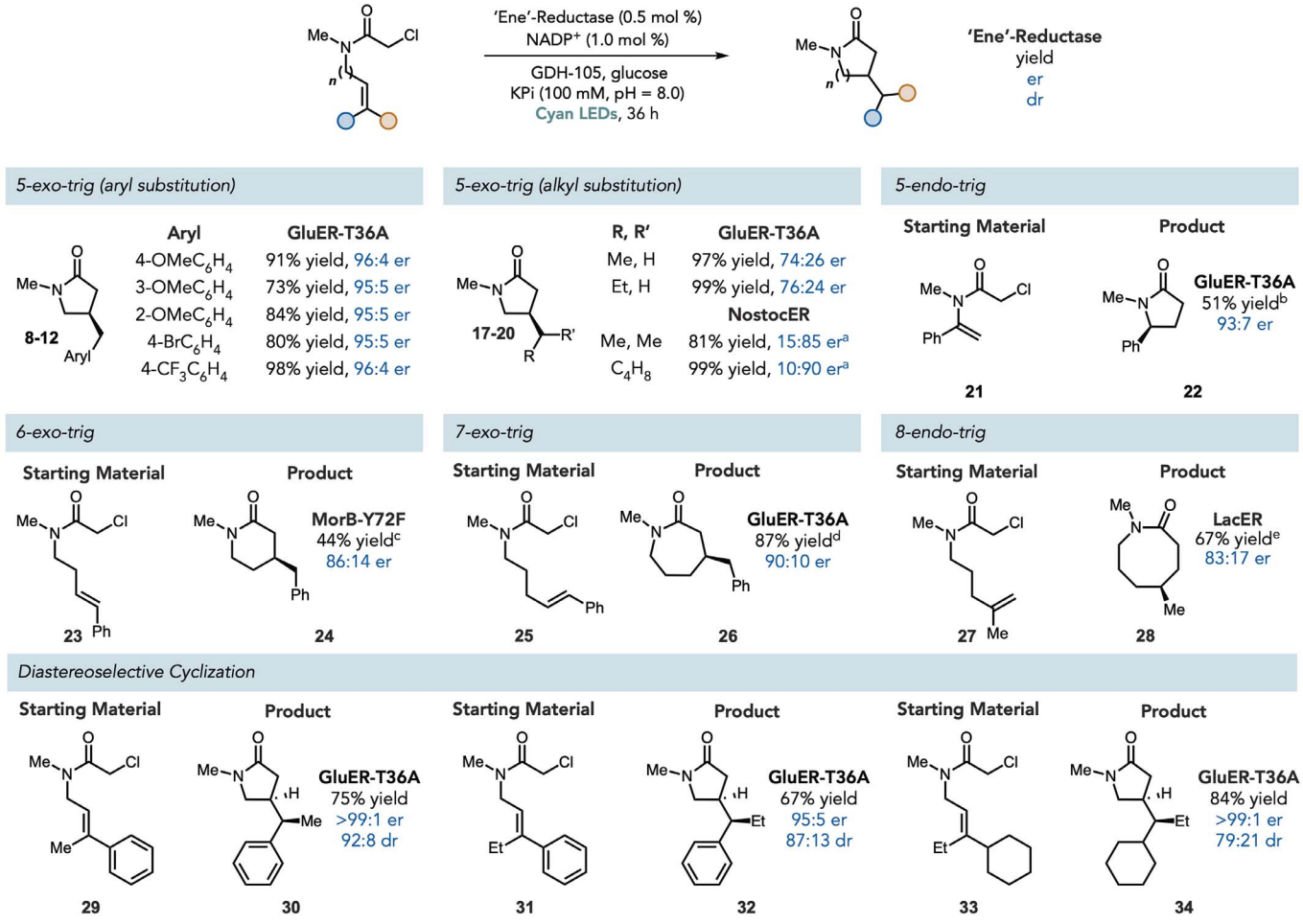

Fig. 2. Scope of the biocatalytic radical cyclization. Reaction conditions: GluER-T36A (0.5 mol %), $NADP^+$ (1 mol %), GDH-105 (0.2 mg/mg starting material), glucose (6 equiv.), KPi (pH = 8.0, 100 mM, with 10% glycerol), and substrate (1 equivalent). 50 W Cyan LED. Average temperature, 35°C. [a]Results obtained by using NostocER and favors the opposite product enantiomer. [b]12% formation of the hydrodehalogenated product. [c]1 mol % enzyme loading (18 hours). [d]2 mol % enzyme loading (18 hours). [e]4 mol % enzyme loading with 8 mol % NAD^+ (72 hours).

phosphate ($NADP^+$), glucose, and glucose dehydrogenase (GDH-105) are required for reactivity (table S1). To increase the activity of GluER for this non-natural function, we conducted mutagenesis and found that mutation of T36, a residue located at the surface of the protein, to alanine (T36A) furnished improved yields of product and only trace quantities of the hydrodehalogenated product (Fig. 1C, entry 3). We solved crystal structures of GluER and GluER-T36A and found no differences in the structure that would explain the improved yield (backbone root mean square deviation of 0.53 Å) (figs. S48 to S52). This mutation does not have a detrimental effect on the native function of this enzyme (fig. S45) and allows the catalyst loading to be decreased to 0.5 mole % (mol %) without compromising yield or enantioselectivity (fig. S46). Moreover, this reaction can be conducted with lyophilized cell-free lysate. This feature enabled the model cyclization to be run on gram scale, providing product with no change in yield or enantioselectivity (Fig. 1C, entry 4). The reaction could be run open to air with slow addition of glucose over 8 hours, providing comparable yields and enantioselectivities to reactions run under inert atmosphere (Fig. 1D). Alternatively, GDH-105, $NADP^+$, and glucose could be replaced with periodic addition of sodium dithionite and degassed buffer; when run open to air, there was no observable change in the reaction outcome (Fig. 1D).

With optimized conditions in hand, we explored the scope and limitations of this reaction (Fig. 2). Aromatic substituted alkenes are tolerated for 5-exo-trig cyclizations, affording product in high yield and enantioselectivity with substituents at the para-, meta-, and ortho positions (Fig. 2, **8-12**). The electronic characteristics of these substituents had only a modest effect on reaction efficiency. Alkyl substituents on the olefin are also tolerated, affording product in nearly quantitative yield in all cases, albeit with diminished enantioselectivities (Fig. 2, **17-20**). Because this mode of reactivity should be accessible across the entire ERED family, we suspected that other members might provide improved levels of enantioselectivity. An ERED from *Nostoc* sp. (NostocER) accordingly provided improved enantioselectivities for the more sterically demanding alkyl-substituted substrates (Fig. 2, **19, 20**).

We next shifted our attention to other cyclization modes. GluER-T36A catalyzes a 5-endo-trig cyclization, in which the stereogenic center is created by means of hydrogen atom transfer (HAT) to yield the 5-substituted γ-lactam (Fig. 2, **22**). The ERED is thus capable of controlling the delivery of a hydrogen atom to sites distal to the carbonyl, a feat largely unknown in the small molecule literature (*10*, *28*). A 6-exo-trig cyclization to furnish δ-lactams occurs with GluER-T36C in modest yield and enantioselectivity. Improved levels of enantioselectivity and yield can be achieved by using a variant of Morphinone reductase (MorB-Y72F) (Fig. 2, **24**). GluER-T36A can also catalyze a 7-exo-trig cyclization (Fig. 2, **26**), albeit with increased catalyst loadings. Last, an 8-endo-trig cyclization is also possible by using GluER-T36A, affording product in high yields but with essentially no enantioselectivity. An ERED from *Lactobacillus casei* (LacER) provides significantly improved levels of enantioselectivity but slightly diminished yields, with the remaining mass balance being unreacted starting material (Fig. 2, **28**). The latter examples are particularly exciting because they are underrepresented cyclization modes in the small molecule literature (*29*).

Inspired by the selectivity of the HAT event, we considered the possibility of ERED-controlled hydrogen atom delivery to exocyclic prochiral radicals. Because these radicals are conformationally flexible, controlling HAT is challenging. We began by testing substrates that possess trisubstituted alkenes for the 5-exo-trig cyclization mode. Substrates that contain phenyl/methyl and phenyl/ethyl substituents at the terminal position of the olefin afforded lactams with excellent enantio- and diastereoselectivities (Fig. 2, **30** and **32**). Because these substrates provide an equimolar mixture of diastereomers when prepared with photoredox catalysts, there does not appear to be a thermodynamic preference for one diastereomer, demonstrating that the enzyme is responsible for controlling the delivery of the hydrogen atom. The cyclohexyl/Et substituted alkene substrate **33**, which lacks an aromatic group, was also a substrate for this reaction, with diastereoselectivity only slightly diminished (Fig. 2, **34**). Substrates that contain substituents with steric bulk may thus be ideal for achieving high levels of diastereoselectivity.

We conducted a series of initial rate experiments to better understand how the kinetic profile of the reaction compares with native alkene reduction. We found that the model reaction follows Michaelis-Menten kinetics with a Michaelis constant (K_m) = 9.7 mM, an apparent unimolecular rate constant (k_{cat}) = 0.012 s^{-1}, and a k_{cat}/K_m of 0.0012 mM^{-1} s^{-1} (fig. S27). On the

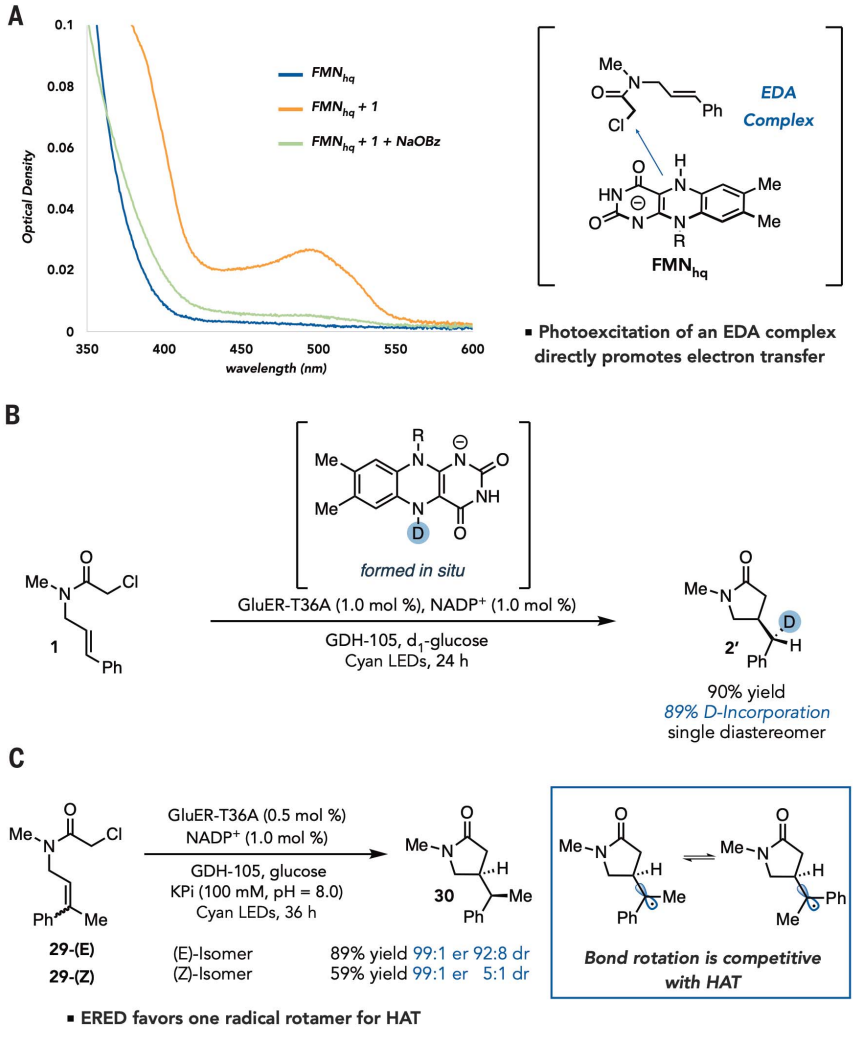

Fig. 3. Mechanistic experiments. (**A**) UV-visible spectrum of reduced GluER-T36A (FMN_{hq}) in the presence of substrate (FMN_{hq} + **1**) and in the presence of substrate and sodium benzoate (FMN_{hq} + **1** + NaOBz). (**B**) Isotope labeling. (**C**) Conformation-selective HAT.

basis of our observation that increased light intensities afford increased rates and higher yields, we suspect that the decreased k_{cat} is due to the reaction being photon limited (fig. S28). We observed a quantum yield of 7.8%.

We conducted a series of mechanistic experiments to better understand the nuances of this reaction, including the superior reactivity with cyan light-emitting diodes (LEDs) [peak maximum (λ_{max}) = 497 nm]. Reduction of GluER to the FMN_{hq} oxidation state with dithionite revealed formation of the diagnostic FMN_{hq} signature with minimal absorption at 497 nm, suggesting that direct excitation of the cofactor is not responsible for the observed wavelength preference (Fig. 3A, FMN_{hq}). Addition of 100 equivalents of chloroamide **1** resulted in formation of a broad absorption band at λ_{max} = 500 nm (Fig. 3A, FMN_{hq} + **1**). Because this absorption feature is not lost upon addition of sodium dithionite, we do not attribute it to FMN_{sq}. It is lost, however, upon addition of 150 equivalents of sodium benzoate (Fig. 3A, FMN_{hq} + **1** + NaOBz). These data are consistent with the formation of an electron donor-acceptor complex between the substrate and FMN_{hq} within the enzyme active site. We propose that excitation of this charge transfer band promotes the initial electron transfer from FMN_{hq} to **1**.

Next, we sought evidence for the existence of radical intermediates by preparing a substrate containing a cyclopropyl ring. GluER-T36A produced only products of cyclopropane ring opening, supporting the existence of a radical intermediate (fig. S9). To determine the terminal hydrogen atom source, we used labeled $FMND_{hq}$ generated in situ from D-glucose-1-d_1 (Fig. 3A). Deuterium was incorporated exclusively at the benzylic carbon, with a high level of diastereocontrol. These experiments support a reaction mechanism in which substrate is initially reduced by one electron after irradiation of the electron donor-acceptor complex formed between the substrate and FMN_{hq} within the enzyme active site. The α-acyl radical can react with the pendent olefin to afford an exocyclic radical that is terminated through hydrogen atom transfer from neutral flavin semiquinone (FMN_{sq}) to afford the product and oxidized flavin (fig. S47).

On the basis of this mechanistic hypothesis, we reasoned that the configuration of the alkene may be responsible for the observed levels of diastereoselectivity if HAT is faster than rotation of the exocyclic C–C bond. We thus performed the reaction on starting material **29** with (Z)-alkene geometry rather than the (E)-isomer. Both alkene geometries favor the same diastereomer and produce no change in the enantioselectivity (Fig. 3C). The enzyme thus favors HAT from one rotamer of the prochiral radical at rates that are competitive with bond rotation. The diminished levels of diastereoselectivity observed with the (Z)-alkene isomer are presumably due to a small degree of hydrogen atom transfer before bond rotation.

Transient absorption spectroscopy with olefin isomers of **29** provides additional support for this mechanistic hypothesis. Initial excitation at 370 nm followed by a broad-band probe pulse reveals underlying dynamics of the flavin redox states. We used a sequential kinetic scheme to fit the data through global analysis. We found three time constants that describe the temporal evolution of the various flavin species through evolutionary associated difference spectra (EADS). When **(E)-29** is used as the substrate, a signal corresponding to the charge transfer state decays in 10 ps to the FMN_{sq}. This time scale is consistent with previously reported rates of decomposition for the α-chloroacetophenone ketyl radical anion (*30*). The neutral FMN_{sq} decays on the time scale of 250 ps to the flavin quinone (FMN_{ox}) (figs. S42 and S43). This decay likely corresponds to the rate of cyclization and termination of the radical through hydrogen atom transfer from FMN_{sq}. When the same experiment is conducted on **(Z)-29**, the FMN_{sq} lifetime increases to 700 ps (figs. S39 and S40). These data are consistent with post-cyclization rotation of the exo-cyclic radical to a conformation in which HAT from the FMN_{sq} to the substrate-centered radical is kinetically facile.

We anticipate that the light-promoted reactivity demonstrated here will be replicable widely in EREDs, KREDs, and other classes of oxidoreductases known in biocatalysis for their promiscuity and adaptability. These flavoenzymes may serve as stereoselective catalysts for unexpected radical transformations beyond those demonstrated here, depending on the active site organization, provided starting material, and properties of the excited state flavin. By more widely investigating and exploiting photoexcited states of cofactors, it should be possible to photoinitiate radical-based reactions within enzymes that are otherwise inaccessible in the ground state.

REFERENCES AND NOTES

1. C. M. Jäger, A. K. Croft, *Chem. Bio. Eng.* **5**, 143–162 (2018).
2. A. Studer, D. P. Curran, *Angew. Chem. Int. Ed.* **55**, 58–102 (2016).
3. U. T. Bornscheuer, R. J. Kazlauskas, *Angew. Chem. Int. Ed.* **43**, 6032–6040 (2004).
4. N. A. Romero, D. A. Nicewicz, *Chem. Rev.* **116**, 10075–10166 (2016).
5. S. Seifert, S. Brakmann, *ACS Chem. Biol.* **13**, 1914–1920 (2018).
6. J. Gao, H. Wang, Q. Yuan, Y. Feng, *Front. Plant Sci.* **9**, 357 (2018).
7. L. Schmermund *et al*., *ACS Catal.* **9**, 4115–4144 (2019).
8. M. Gabruk, B. Mysliwa-Kurdziel, *Biochemistry* **54**, 5255–5262 (2015).
9. D. Sorigué *et al*., *Science* **357**, 903–907 (2017).
10. A. Sancar, *Chem. Rev.* **103**, 2203–2237 (2003).
11. M. A. Emmanuel, N. R. Greenberg, D. G. Oblinsky, T. K. Hyster, *Nature* **540**, 414–417 (2016).
12. K. F. Biegasiewicz, S. J. Cooper, M. A. Emmanuel, D. C. Miller, T. K. Hyster, *Nat. Chem.* **10**, 770–775 (2018).
13. K. Hung, X. Hu, T. J. Maimone, *Nat. Prod. Rep.* **35**, 174–202 (2018).
14. M. P. Sibi, S. Manyem, J. Zimmerman, *Chem. Rev.* **103**, 3263–3296 (2003).
15. Y. Cai, B. P. Roberts, D. A. Tocher, *J. Chem. Soc., Perkin Trans. 1* (11): 1376–1386 (2002).
16. E. Vitaku, D. T. Smith, J. T. Njardarson, *J. Med. Chem.* **57**, 10257–10274 (2014).
17. S. P. France *et al*., *ACS Catal.* **6**, 3753–3759 (2016).
18. D. P. Curran, J. Tamine, *J. Org. Chem.* **56**, 2746–2750 (1991).
19. K. Hiroi, M. Ishii, *Tetrahedron Lett.* **41**, 7071–7074 (2000).
20. N. G. Schmidt, E. Eger, W. Kroutil, *ACS Catal.* **6**, 4286–4311 (2016).
21. N. J. Turner, E. O'Reilly, *Nat. Chem. Biol.* **9**, 285–288 (2013).
22. H. S. Toogood, N. S. Scrutton, *ACS Catal.* **8**, 3532–3549 (2018).
23. K. Heckenbichler *et al*., *Angew. Chem. Int. Ed.* **57**, 7240–7244 (2018).
24. B. A. Sandoval, A. J. Meichan, T. K. Hyster, *J. Am. Chem. Soc.* **139**, 11313–11316 (2017).
25. J. J. Warren, M. E. Ener, A. Vlček Jr., J. R. Winkler, H. B. Gray, *Coord. Chem. Rev.* **256**, 2478–2487 (2012).
26. S. Ghisla, V. Massey, J.-M. Lhoste, S. G. Mayhew, *Biochemistry* **13**, 589–597 (1974).
27. V. Massey, P. Hemmerich, W. R. Knappe, H. J. Duchstein, H. Fenner, *Biochemistry* **17**, 9–16 (1978).
28. Z. G. Brill, H. K. Grover, T. J. Maimone, *Science* **352**, 1078–1082 (2016).
29. L. Yet, *Tetrahedron* **55**, 9349–9403 (1999).
30. D. D. Tanner, J. J. Chen, L. Chen, C. Luelo, *J. Am. Chem. Soc.* **113**, 8074–8081 (1991).

ACKNOWLEDGMENTS

We thank M. Souza for preparing glassware for spectroscopy studies, C. Kraml and L. Wilson at Lotus Separations for compound purification, P. Jeffrey for assistance with x-ray structure determination, K. Conover for assistance in photoNMR data acquisition, and the staff of NSLS-II beamline FMX (17-ID-2) for help with data collection. **Funding:** Research reported in this publication was supported by the National Institutes of Health (NIH) National Institute of General Medical Sciences (NIGMS) (R01 GM127703), the Searle Scholars Award (SSP-2017-1741), Sloan Research Fellowship, the Princeton Catalysis Initiative, and Princeton University. D.G.O. acknowledges support from the Postgraduate Scholarships Doctoral Program of the Natural Sciences and Engineering Research Council of Canada. D.G.O. and G.D.S. acknowledge support from the Division of Chemical Sciences, Geosciences, and Biosciences, Office of Basic Energy Sciences of the U.S. Department of Energy (DOE) through grant DE-SC0019370. The AMX (17-ID) beamline of The Life Science Biomedical Technology Research (LSBR) resource is primarily supported by NIH, NIGMS through a Biomedical Technology Research Resource P41 grant (P41GM111244), and by the DOE Office of Biological and Environmental Research (KP1605010). As a National Synchrotron Light Source II facility resource at Brookhaven National Laboratory, work performed at LSBR is supported in part by the DOE Office of Science, Office of Basic Energy Sciences Program under contract DE-SC0012704 (KC0401040). **Author contributions:** T.K.H. conceived and directed the project. T.K.H., K.F.B., S.J.C., X.G., and J.H.K. designed the experiments. K.F.B., S.J.C., X.G., and J.H.K. performed and analyzed results. B.A.S. cloned the improved variant, and S.E.G. obtained x-ray quality crystals and solved the crystal structures. L.A.J. determined the absolute configuration. D.G.O. designed and conducted the spectroscopic studies, and D.G.O. and G.D.S. analyzed the data. **Competing interests:** The authors declare no conflicts of interest. **Data and materials availability:** All data are available in the main text or the supplementary materials. Crystallographic models and structure factors have been deposited in the Protein Data Bank with accession nos. 6O08 and 6MYW for GluER and GluER-T36A, respectively. X-ray crystallographic data for lactam **2** have been deposited in the Cambridge Crystallographic Data Centre (1878605).

SUPPLEMENTARY MATERIALS

science.sciencemag.org/content/364/6446/1166/suppl/DC1
Materials and Methods
Figs. S1 to S52
Tables S1 to S3
References (*31*–*56*)

7 December 2018; accepted 29 May 2019
10.1126/science.aaw1143

Photoexcitation of flavoenzymes enables a stereoselective radical cyclization

Kyle F. Biegasiewicz, Simon J. Cooper, Xin Gao, Daniel G. Oblinsky, Ji Hye Kim, Samuel E. Garfinkle, Leo A. Joyce, Braddock A. Sandoval, Gregory D. Scholes and Todd K. Hyster

Science **364** (6446), 1166-1169.
DOI: 10.1126/science.aaw1143

Light teaches (co)enzymes new tricks

Light is widely used in organic synthesis to excite electrons in a substrate or catalyst, opening up reactive pathways to a desired product. Biology uses light sparingly in this way, but coenzymes such as flavin can be driven to excited states by light. Biegasiewicz *et al.* investigated this reactivity and found a suite of flavoenzymes that catalyze asymmetric radical cyclization when exposed to light. "Ene"-reductases, when reduced and illuminated, converted starting materials containing an α-chloroamide and an alkene into five-, six-, seven-, or eight-membered lactams. Different enzymes furnished different stereochemistry in the products, likely because of changes in active-site pocket geometry.

Science, this issue p. 1166